



<http://www.diva-portal.org>

## Postprint

This is the accepted version of a paper published in *Crystal Growth & Design*. This paper has been peer-reviewed but does not include the final publisher proof-corrections or journal pagination.

Citation for the original published paper (version of record):

Svärd, M., Nordström, F L., Jasnobulka, T., Rasmuson, Å C. (2010)  
Thermodynamics and Nucleation Kinetics of m-Aminobenzoic Acid Polymorphs.  
*Crystal Growth & Design*, 10(1): 195-204  
<http://dx.doi.org/10.1021/cg900850u>

Access to the published version may require subscription.

N.B. When citing this work, cite the original published paper.

Permanent link to this version:

<http://urn.kb.se/resolve?urn=urn:nbn:se:kth:diva-10500>

# Thermodynamics and Nucleation Kinetics of m-Aminobenzoic Acid Polymorphs

Michael Svärd, Fredrik L. Nordström<sup>†</sup>, Tanja Jasnobulka and Åke C. Rasmuson<sup>\*,‡</sup>

Dept. of Chemical Engineering and Technology, Royal Institute of Technology, Stockholm, Sweden.

<sup>\*</sup>) To whom correspondence should be addressed. E-mail: ake.rasmuson@ul.ie.

<sup>†</sup>) Abbott Laboratories, North Chicago, IL, USA.

<sup>‡</sup>) Current address: Dept. of Chemical and Environmental Science, Materials and Surface Science Institute, University of Limerick, Limerick, Rep. of Ireland.

## OPEN ACCESS VERSION DECLARATION

This is the accepted version of the following article:

Svärd, M, F.L. Nordström, T. Jasnobulka and Å.C. Rasmuson; *Cryst. Growth Des.* **10**(1), 195-204 (2010), which has been published in final form at:

<http://pubs.acs.org/doi/abs/10.1021/cg900850u>

**ABSTRACT.** The polymorphism of m-aminobenzoic acid has been investigated. Two polymorphs have been identified and characterized by XRPD, FTIR, microscopy and thermal analysis. The melting properties and isobaric heat capacities of both polymorphs have been determined calorimetrically, and the solubility of each polymorph in several solvents at different temperatures has been determined gravimetrically. The solid-state activity (i.e. the Gibbs free energy of fusion) of each polymorph has been determined through a comprehensive thermodynamic analysis based on experimental data. It is found that the polymorphs are enantiotropically related, with a stability transition temperature of 156.1°C. The published crystal structure belongs to the polymorph that is metastable at room temperature. Energy-temperature diagrams of both polymorphs have been established by determining the free energy, enthalpy and entropy of fusion as a function of temperature. A total of 300 cooling crystallizations have been carried out at constant cooling rate using different saturation temperatures and solvents, and the visible onset of primary nucleation recorded. The results show that for this substance, the polymorph that will nucleate depends chiefly on the solvent. In water and methanol solutions, the stable form I was obtained in all experiments, whereas in acetonitrile, a majority of nucleation experiments resulted in the isolation of the metastable form II. It is shown how this can be rationalised by analysis of solubility, solution speciation and nucleation relationships. The importance of carrying out multiple experiments at identical conditions in nucleation studies of polymorphic systems is demonstrated.

## INTRODUCTION

When crystallizing pharmaceuticals it is necessary to take into account the phenomenon of polymorphism, or the existence of more than one distinct crystal structure of a single compound. About one third of all active pharmaceutical ingredients are confirmed polymorphic systems<sup>1</sup>, and a similar number has been reported for organic compounds in general<sup>2</sup>. The difference between polymorphs in properties such as solubility, dissolution rate and bioavailability has prompted regulatory requirements stating that possible polymorphs of active pharmaceutical ingredients must be identified<sup>3</sup>.

The various substituted benzoic acids form an interesting group of molecules with a wide range of pharmaceutical connotations, and many of these substances exhibit polymorphism. The substance meta-aminobenzoic acid – mABA (figure 1) – is of considerable importance in the pharmaceutical industry, e.g. in the synthesis of analgesics, as well as in other branches of the chemical industry<sup>4</sup>, and it possesses some interesting properties as a simple model molecule with complex hydrogen bonding abilities.

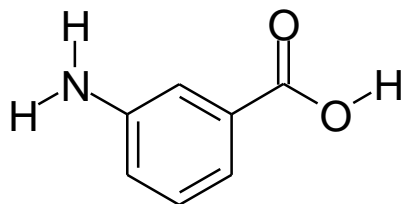


**Figure 1.** Schematic molecular structure of meta-aminobenzoic acid.

Only one crystal structure has been published<sup>5</sup>, but spectroscopic work in the 60's and 70's<sup>6,7</sup> has described the existence of a second form, reported to be zwitterionic. If this is the case, mABA would be similar to its ortho-isomer (anthranilic acid), which has been shown to possess one zwitterionic polymorph as well as two non-ionic forms.

In the present study, the polymorphism of mABA is examined in detail. Experimental work confirms the existence of two polymorphs, and thermodynamic data as well as nucleation experiments are reported.

## EXPERIMENTAL WORK

### *Materials*

m-Aminobenzoic acid (CAS reg. no. 99-05-8,  $M_w$ =137.14 g/mol) was purchased from Sigma-Aldrich (purity > 98%) and used with no further purification steps. Solvents were purchased from VWR: Ethyl acetate (HiperSolv >99.8%), Acetonitrile (LiChrosolv >99.8%), Methanol (p.a. >99.9%), Acetone (HiperSolv >99.8%). In addition, deionised and microfiltered (pore size 0.2  $\mu$ m) water was used.

### *Polymorph identification and preparation*

ATR-FTIR spectroscopy and XRPD have been used for the identification and characterization of the polymorphs of mABA. For the infrared spectroscopy, a Perkin Elmer Instruments Spectrum One with an attenuated total reflectance (ATR) module, equipped with a ZnSe-crystal window, was employed, using a scanning range of 650 - 4000  $\text{cm}^{-1}$ . XRPD patterns were recorded using a X'Pert PRO diffractometer, equipped with a theta/theta goniometer, using  $\text{CuK}\alpha$ -radiation.

Crystals of mABA were grown by controlled solvent evaporation, using perforated plastic film-coated glass containers with saturated solutions, for the purpose of growing crystals of sufficient size for structure determination with single crystal XRD.

### *Thermal analysis*

The melting temperatures and corresponding melting enthalpies of the polymorphs of mABA have been obtained by differential scanning calorimetry (DSC), using a TA Instruments DSC 2920 with

hermetically sealed aluminium pans. Heating rates between 2 - 5 K/min were used. The instrument was calibrated against the melting properties of indium.

The isobaric, specific heat capacity of the pure polymorphs ( $C_p$ ) was determined with modulated DSC, using the same instrument. Non-hermetic sample pans were used in order to improve the accuracy. A modulation period of 100 s and an amplitude of 1°C were employed, together with a constant heating rate of 3°C/min preceded by an initial isothermal period of 10 min. Pans were selected so as to limit the difference in weight between sample pan and reference pan to 0.20 mg. The instrument was calibrated according to standard procedure against the melting properties of indium, and the heat capacity signal was calibrated with three runs of a sapphire sample in the relevant temperature interval. A linear calibration curve rather than a calibration constant was used, based on the average of the three sapphire sample runs.

### *Solubility*

The solubility has been determined gravimetrically, insofar as it has been feasible, in a variety of solvents for two polymorphs of mABA. Solutions of mABA were prepared in sealed 250 ml and 500 ml bottles and agitated with PTFE-coated magnetic bars. The crystals used for the solutions were either the purchased material or crystals obtained by rapid cooling of solutions saturated at higher temperatures. The solutions containing excess solid crystalline material of the specified polymorph (verified with FTIR) were allowed to equilibrate by dissolution under agitation, at different temperatures ranging from 0 - 50°C in increments of 5°C. The temperature was controlled with Julabo FP-50 thermostatic bath to within 0.01°C. The temperature in the cryostat was validated using a mercury calibration thermometer (Thermo-Schneider, Wertheim, Germany, accuracy of 0.01°C). Samples of solution were collected using pre-heated syringes with filters (0.2 µm; CA for aqueous solutions, otherwise PTFE) and the sample mass recorded directly, with a precision of 0.0001 g. Solutions were allowed some sedimentation before sampling, as this was found to enhance the reproducibility. The samples were dried in a ventilated laboratory hood, with the mass monitored regularly, until completely dry. The solubility was calculated from the registered masses. Multiple samples from multiple solutions were collected to ensure that equilibrium had been attained as well as to minimize experimental error.

### *Primary nucleation*

Saturated solutions (with respect to the stable polymorph) prepared in 500 ml bottles at 45 and 55°C, respectively, were filtered into sealed test tubes (15 ml), agitated with PTFE-coated magnetic bars, using pre-heated syringes with filters 0.2 µm; CA or PTFE), in batches of 30 test tubes. Each batch of test tubes were kept in a thermostatic bath at 60°C for 24 h in order to remove any resident solution memory of the structure of the dissolved material. The test tubes were subsequently cooled at a constant cooling rate of 10°C/h, while being recorded using a digital Sony DCR-SR72e camcorder. The onset of nucleation was then determined visually with an estimated accuracy of 0.1°C. As soon as sufficient crystal material had precipitated in a given test tube, the content was filtered using Munktell grade 1003 filter paper, and ATR-FTIR spectroscopy was used to identify the crystallized polymorph. Filtration and analysis was done as quickly as was experimentally feasible in order to reduce the risk of solvent-mediated transformation of the crystalline material. The initial concentration of each flask was measured gravimetrically with the same method as for the solubility determinations.

## RESULTS

### *Polymorph identification*

Crystals grown from evaporation of ethyl acetate or acetonitrile exhibited a needle- or rod-like habit, with crystals sometimes exceeding 1 mm in length. One such crystal was analysed with single crystal XRD, and the structure proved to be identical to the one published in 1980 by Voogd et al.<sup>5</sup>, present in the Cambridge Structural Database with refcode AMBNZA. This polymorph will be referred to as form II. Analysis with IR spectroscopy for this polymorph rendered a spectrum with significant differences from that obtained using the purchased crystal material, which is henceforth termed form I. IR spectra

of the two polymorphs are shown in figure 2. Crystals grown from evaporation of methanol, water or acetone proved on IR analysis to be form I. Unfortunately, no crystals could be grown with adequate size for analysis with single crystal XRD. XRPD on crystalline powder of forms I and II, shown in figure 3, rendered final proof of the existence of two distinct crystal structures.

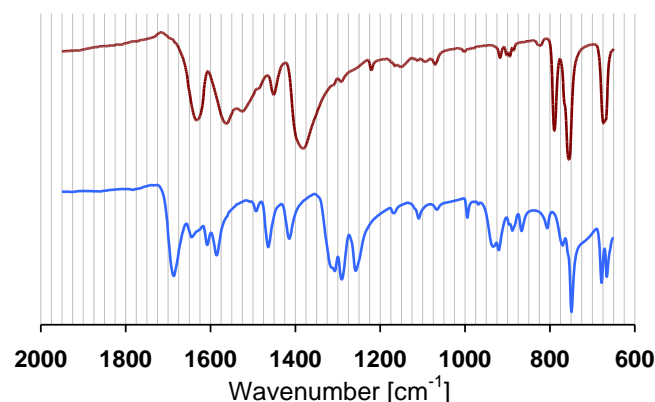


**Figure 2.** IR spectra of the two polymorphs of mABA: Form I (red, upper) and form II (blue, lower).

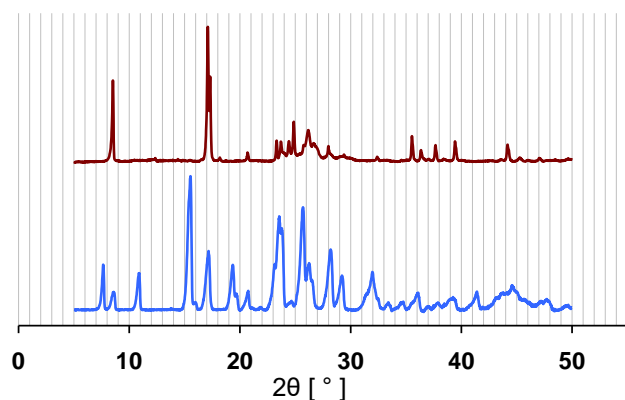


**Figure 3.** XRPD diffractograms of the two polymorphs of mABA: Form I (red, upper) and form II (blue, lower).

Figure 4 shows microscope images of crystals of the two polymorphs, obtained by slow evaporation of water (form I) and ethyl acetate (form II). Form I shows dendritic growth, forming small cascades of threads, possibly due to twinning, whereas form II develops needle-like crystals which may grow to several millimetres in length.

#### *Thermal analysis*

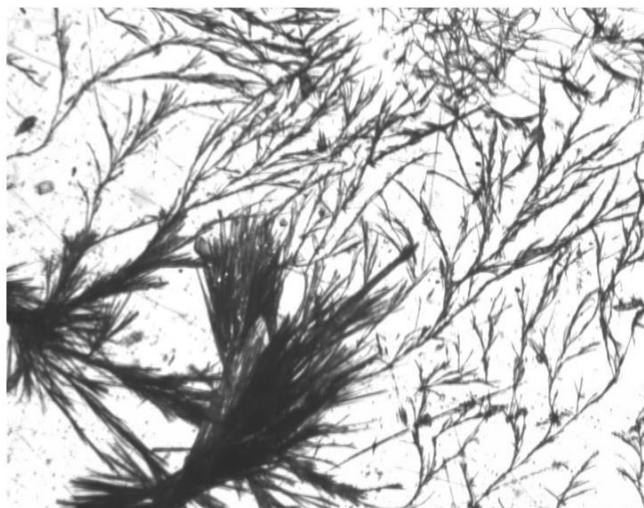
The melting point,  $T_m$ , enthalpy and entropy of fusion,  $\Delta H^f$  and  $\Delta S^f$ , respectively, of the two polymorphs are given in table 1. All samples were subjected to polymorph verification with ATR-FTIR, and the polymorphic purity was confirmed by DSC.

**Table 1.** Melting data of polymorph I and II with 95% confidence limits.

polymorph	scans	$T_m^a/^\circ\text{C}$	$\Delta H^f(T_m)/\text{kJ}\cdot\text{mol}^{-1}$	$\Delta S^f(T_m)/\text{J}\cdot\text{K}^{-1}\cdot\text{mol}^{-1}$
I	6	$172.04 \pm 0.25$	$35.51 \pm 1.14$	79.76
II	9	$177.98 \pm 0.46$	$26.74 \pm 0.70$	59.27

a) extrapolated onset temperature

a) Form I



b) Form II

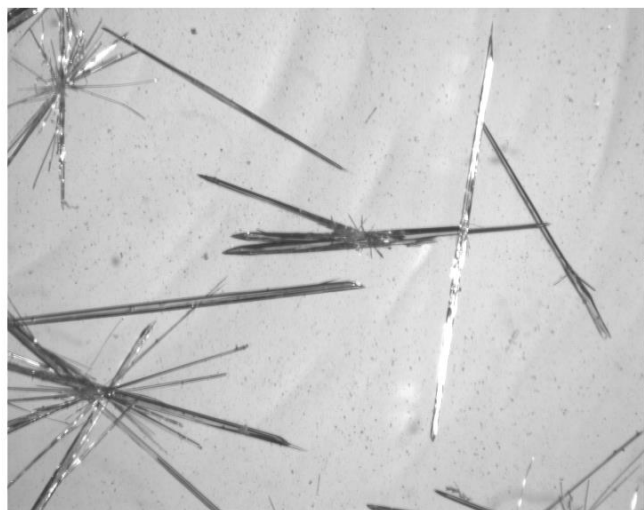


**Figure 4.** Microscope pictures of crystals of a) form I and b) form II.

Four DSC thermograms of mABA are shown in figure 5. Thermograms A and B show the two polymorphs melting without any prior solid-solid transformation; a typical result when using pure material. Thermogram C shows how the starting polymorph I melts, followed by an immediate recrystallization into form II, which subsequently melts, and thermogram D shows a solid-solid endothermic transformation of form I into form II, which then melts, both less common occurrences, possibly induced by small traces of form II being present. Only thermograms of type A or B were used for the melting data in table 1.

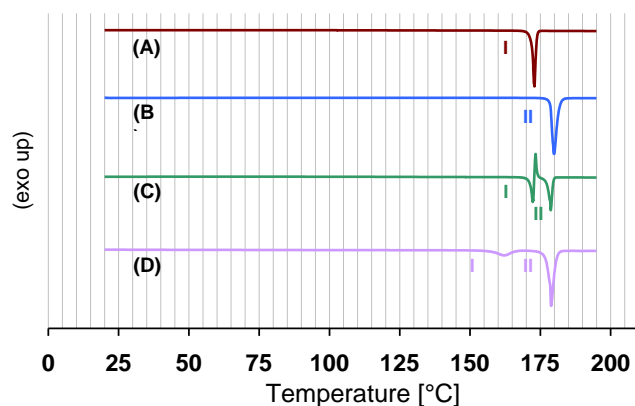


**Figure 5.** DSC thermograms of mABA polymorphs: A (red) – form I melts; B (blue) – form II melts; C (green) – form I melts, form II recrystallizes and then melts; D (purple) – form I transforms into form II which then melts.

The specific heat capacity of the two polymorphs was determined in the temperature interval 300 - 400 K. The material used was the purchased material (form I) and crystals obtained by rapid cooling crystallizations of ethyl acetate solutions (form II). All samples were subjected to polymorph verification with ATR-FTIR. Using a linear regression model on the form:

$$C_p = k_1 + k_2 T \quad (1)$$

the coefficients  $k_1$  and  $k_2$  were determined by a least-squares fit of all the  $C_p$ -data from multiple scans for each polymorph at different temperatures. The heat capacity of the melt could not be determined due to significant evaporation upon melting. No suspected polymorphic transformation was observed during the heat capacity measurements. A total of 19 scans were carried out. Two scans (one for each polymorph) were disregarded, as the resulting heat capacity – temperature plots deviated greatly with respect both to slope and displacement from the remaining set, presumably due to poor contact between the sample pan and the DSC cell.

The heat capacity coefficients are summarized in table 2.

**Table 2.** Heat capacity coefficients of eq. 1 for the two polymorphs.

polymorph	scans	T-interval/K	$k_1/\text{J}\cdot\text{K}^{-1}\cdot\text{mol}^{-1}$	$k_2/\text{J}\cdot\text{mol}^{-1}$
I	8	300 - 400	39.60	0.4825
II	9	300 - 400	41.54	0.5237

### *Solubility*

The solubility of form I was determined at five degree intervals from 10 - 50°C in water, acetonitrile, ethyl acetate and methanol. The true solubility of form II was successfully determined at low temperatures in acetonitrile and ethyl acetate. A gradual transformation into form I slightly above room temperature precluded further solubility measurements of form II in these solvents. In water and methanol, no crystals of form II could be obtained by rapid cooling crystallization, and as crystals introduced into solution transformed rapidly into form I in these solvents, no solubility measurements were feasible. Solubility data is presented in table 3.

**Table 3.** Solubility of the two mABA polymorphs, reported as averages with 95% confidence limits, and the number of samples given in brackets.

T/°C	solubility [no. of samples] given in g mABA per kg solvent					
	<i>form I</i>			<i>form II</i>		
	water	acetonitrile	ethyl acetate	methanol	acetonitrile	ethyl acetate
0	-	-	-	-	-	19.34 ± 0.66 [6]
5	-	-	-	-	14.20 ± 0.45 [2]	21.10 ± 0.10 [12]
10	3.50 ± 0.16 [4]	5.27 ± 0.07 [4]	6.71 ± 0.21 [4]	38.56 ± 0.05 [4]	16.82 ± 0.04 [6]	24.06 ± 0.19 [7]
15	4.07 ± 0.20 [4]	5.92 ± 0.08 [4]	7.66 ± 0.30 [4]	44.31 ± 0.45 [4]	20.26 ± 0.18 [6]	26.52 ± 0.16 [9]
20	4.66 ± 0.17 [4]	7.15 ± 0.06 [4]	8.78 ± 0.27 [4]	51.73 ± 0.38 [4]	23.39 ± 0.05 [6]	29.61 ± 0.11 [6]
25	5.40 ± 0.15 [4]	9.45 ± 0.31 [6]	10.50 ± 0.35 [8]	60.74 ± 0.80 [4]	27.39 ± 0.07 [4]	33.49 ± 0.24 [8]
30	6.24 ± 0.13 [4]	11.31 ± 0.07 [4]	13.02 ± 0.67 [8]	73.63 ± 0.16 [2]	-	36.53 ± 0.19 [8]
35	7.30 ± 0.16 [4]	15.01 ± 0.38 [8]	15.28 ± 0.54 [8]	88.05 ± 1.46 [8]	-	-
40	8.58 ± 0.08 [4]	18.85 ± 1.12 [8]	18.42 ± 0.35 [8]	100.51 ± 0.85 [6]	-	-
45	10.10 ± 0.12 [4]	22.64 ± 0.67 [8]	21.49 ± 0.52 [4]	118.12 ± 1.40 [4]	-	-
50	11.80 ± 0.11 [6]	27.95 ± 0.64 [8]	26.18 ± 1.02 [4]	138.55 ± 3.15 [4]	-	-

The following regression model was fitted to the solubility data, for each solvent and polymorph:

$$\ln x_{\text{eq}} = AT^{-1} + B + CT \quad (2)$$

where  $x_{\text{eq}}$  is the mole fraction solubility and T the temperature in Kelvin. The coefficients A, B and C were determined using the software Origin 6.1. They are listed, together with the goodness of fit as given by  $\chi^2$ , in table 4. The measured solubility and the regression model are shown in figure 6.

**Table 4.** Coefficients of eq. 2 for the two polymorphs in various solvents.

polymorph, solvent	A	B	C	$\chi^2$
form I, water	1957.08	-29.22	0.05168	$0.03 \cdot 10^{-3}$
form I, acetonitrile	2604.92	-36.07	0.07193	$1.87 \cdot 10^{-3}$
form I, ethyl acetate	2471.76	-31.57	0.06134	$0.48 \cdot 10^{-3}$
form I, methanol	-279.14	-11.93	0.02891	$0.31 \cdot 10^{-3}$
form II, acetonitrile	-4464.59	16.47	-0.02117	$0.09 \cdot 10^{-3}$
form II, ethyl acetate	-242.26	-8.55	0.01841	$0.14 \cdot 10^{-3}$

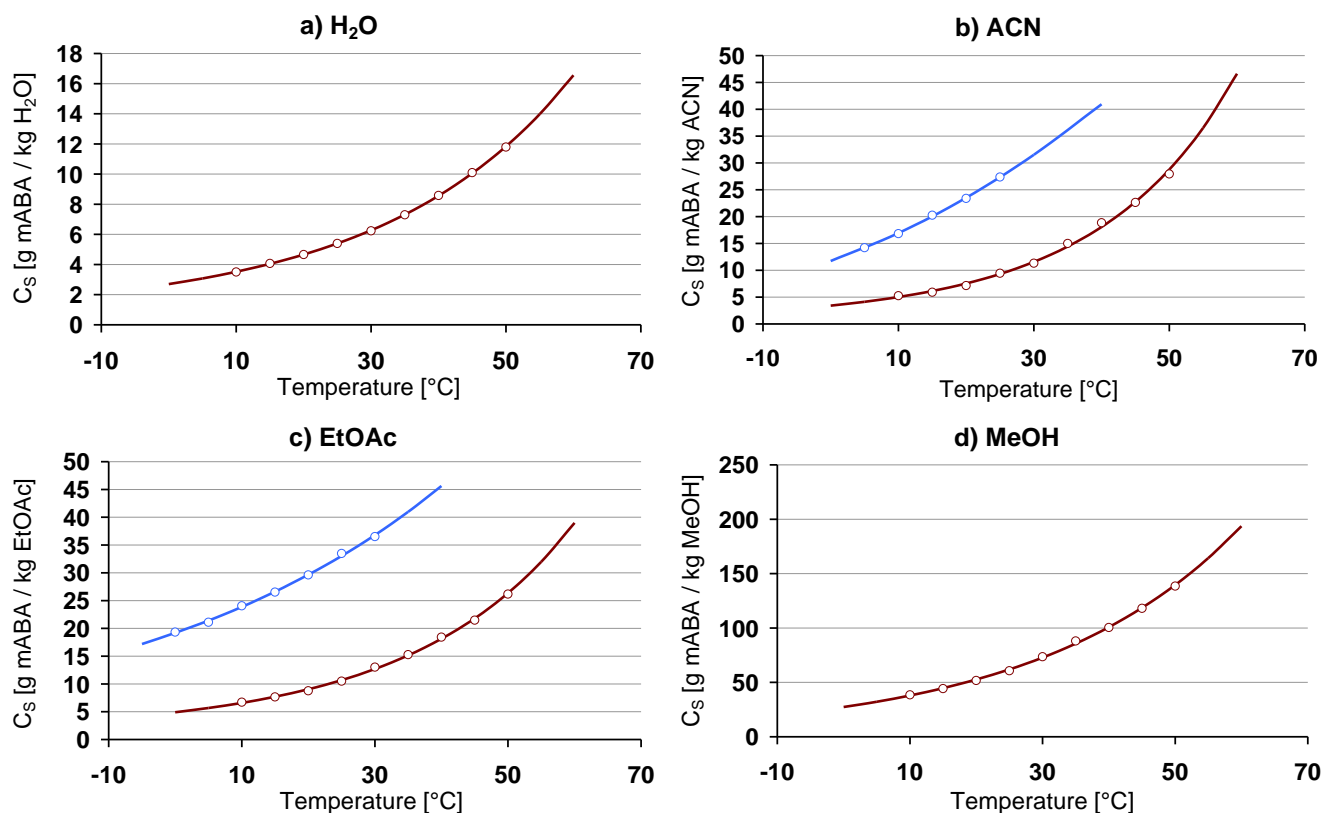


**Figure 6.** Experimentally measured solubility data of mABA form I (red) and form II (blue, where determined) is shown together with corresponding regression curves, for a) water, b) acetonitrile, c) ethyl acetate and d) methanol.

#### Primary nucleation

Table 5 summarizes the nucleation experiments performed under various conditions, the resulting isolated polymorph and the metastable zone widths. In water and methanol, only form I is found. None of the test tubes containing ethyl acetate solution saturated at 45°C nucleated during cooling. Attempts to start with ethyl acetate solutions saturated at 55°C resulted in precipitation of a reaction product, which formed when solutions were kept for some time at high temperatures. In acetonitrile, the majority of experiments produced form II.

**Table 5.** Nucleation experiment results: fraction of samples identified as form I, II or a mixture of both forms, the average metastable zone width with reference to the solubility of form I, and average supersaturation ratio with respect to the observed polymorph at visible onset of nucleation, given with 95% confidence intervals.

solvent	$T_{\text{sat}}/^{\circ}\text{C}$	number of exp <sup>a</sup>	fraction of exp resulting in [%]			MZW/ $^{\circ}\text{C}$	avg $S_I$	avg $S_{II}$
			form I	form II	both I+II			
water	45	60	100	0	0	$38.1 \pm 1.0$	$3.29 \pm 0.10$	
water	55	60	100	0	0	$34.7 \pm 0.8$	$2.86 \pm 0.07$	
acetonitrile	45	60	10	83	7	$39.9 \pm 0.4$	$5.38 \pm 0.08$	$1.58 \pm 0.02$
methanol	45	60	100	0	0	$21.6 \pm 0.9$	$2.01 \pm 0.06$	
ethyl acetate	45	60	-	-	-	$> 48$	$> 4.86$	$> 1.25$

a) number of identical experiments performed under each set of conditions

## ANALYSIS AND DISCUSSION

### *Thermodynamic stability analysis*

The determined solubility data of the two polymorphs in acetonitrile and ethyl acetate, combined with the observed polymorphic transformations in solution from form II into form I shows that form I is thermodynamically stable at ambient conditions. These results in conjunction with the experimentally determined melting properties of the two polymorphs show that the system is enantiotropic. Occasional DSC scans starting with form I resulted in a solid-solid transformation into form II below the melting temperature of form I (see figure 5, thermogram D). This transition was endothermic, which is in accordance with the heat-of-transition rule-of-thumb<sup>8</sup>. The earliest detected extrapolated onset temperature of the solid-solid transition was 157.25°C, which, given a certain kinetic hysteresis, constitutes an upper experimental limit of the transition temperature.

The thermodynamic stability relationship of the two polymorphs over a given temperature interval can be resolved by determining the activity of the two solid phases. In chemical engineering literature, the convention is to take the pure compound as a hypothetical, supercooled melt at the temperature of interest as the reference state. The activity of the solid phase,  $a$ , using this reference state, is then equal to the difference between the chemical potential of the solid and of the pure melt divided by  $RT$ <sup>9</sup>, which can be written, completely rigorously, as:

$$\ln a = \frac{\mu_{\text{solid}} - \mu_{\text{liquid}}}{RT} = \frac{\Delta H^f(T_m)}{R} \left[ \frac{1}{T_m} - \frac{1}{T} \right] - \frac{1}{RT} \int_{T_m}^T \Delta C_p dT + \frac{1}{R} \int_{T_m}^T \frac{\Delta C_p}{T} dT \quad (3)$$

where  $\mu$  denotes chemical potential,  $T_m$  and  $\Delta H^f(T_m)$  the melting temperature and enthalpy of fusion at the melting temperature, respectively, and  $\Delta C_p$  is the difference in specific heat capacity between the supercooled melt and the solid.

Since melting data for both polymorphs of mABA are available in table 1, only the  $\Delta C_p$ -terms in eq. 3 are required for the determination of the activity of the solid. In a previous contribution<sup>9</sup>, a procedure to simultaneously determine the activity of the solid phase and  $\Delta C_p$  was presented, based on the correlation between the so-called van't Hoff enthalpy of solution and the molar solubility in several solvents at each temperature. This correlation is shown in figure 7, for form I of mABA in three solvents.

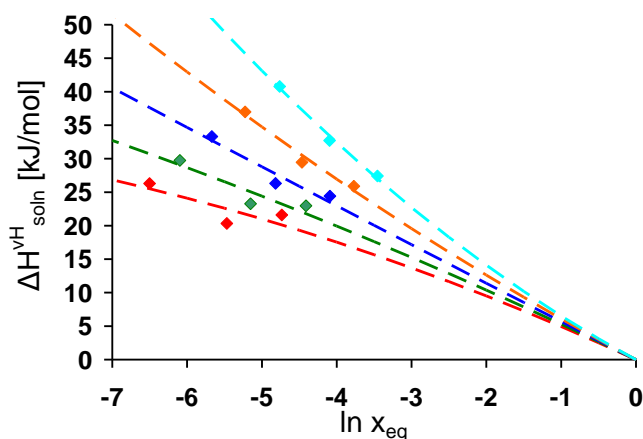


**Figure 7.** Relation between the mole fraction solubility and the solubility temperature dependence of form I, in methanol, acetonitrile and ethyl acetate, for five different temperatures: 10°C (red), 20°C (green), 30°C (blue), 40°C (orange) and 50°C (cyan).

The regression curves in figure 7 were established based on the thermodynamically derived regression equation<sup>10</sup>:

$$\Delta H_{\text{soln}}^{\text{vH}} = \alpha (\ln x_{\text{eq}})^2 + \beta \ln x_{\text{eq}} \quad (4)$$

where  $\alpha$  and  $\beta$  are given in table 6.

**Table 6.** Regression coefficients of eq. 4 for form I (in J/mol).

T/°C	$\alpha$	$\beta$	R <sup>2</sup>
10	-183.6	-5121	0.622
15	-147.6	-5260	0.740
20	-103.5	-5399	0.827
25	-49.1	-5537	0.887
30	18.6	-5670	0.928
35	103.4	-5791	0.955
40	210.8	-5895	0.973
45	348.2	-5969	0.985
50	526.0	-5999	0.992

In the approach to determine the activity of the solid via the correlations shown in figure 7 it is possible to adopt different approximations of the temperature dependence of  $\Delta C_P$ . In this work, a linear dependence according to eq. 5 is assumed, which has been found to be sufficient in previous work<sup>9</sup>. For comparison, a constant value of  $\Delta C_P$  according to eq. 6 has also been evaluated.

$$\Delta C_P = q + r(T_m - T) \quad (5)$$

$$\Delta C_P = q \quad (6)$$

The heat capacity coefficients in eq. 5 and 6 of form I were calculated based on the numerical values of  $\alpha$  and  $\beta$  in table 6, using the aforementioned procedure to determine the activity of the solid phase<sup>9</sup>. Knowing  $\Delta C_P$  of form I as a function of temperature, we may determine the corresponding  $\Delta C_P$  of form II using the solid state heat capacity data of form I and II (table 2). The calculated  $\Delta C_P$  coefficients in eq. 5 and 6 for both polymorphs are given in table 7.

**Table 7.** Coefficients of eq. 5 and 6 for both polymorphs.

polymorph	$\Delta C_P$ -approximation	$q/\text{J}\cdot\text{K}^{-1}\cdot\text{mol}^{-1}$	$r/\text{J}\cdot\text{mol}^{-1}$
form I	$\Delta C_P = q + r(T_m - T)$	146.5	-0.3502
form I	$\Delta C_P = q$	116.5	
form II	$\Delta C_P = q + r(T_m - T)$	128.1	-0.3090
form II	$\Delta C_P = q$	96.0	

Using the  $\Delta C_P$ -approximation given by eq. 5 results in smaller residuals than using eq. 6 and the systematic deviations with temperature are also weaker, which is in accordance with analyses made on other compounds<sup>9</sup>.

Experimental heat capacity values of the two polymorphs, as well as the heat capacity of the supercooled melt calculated using eq. 5 and table 7, are shown in figure 8.

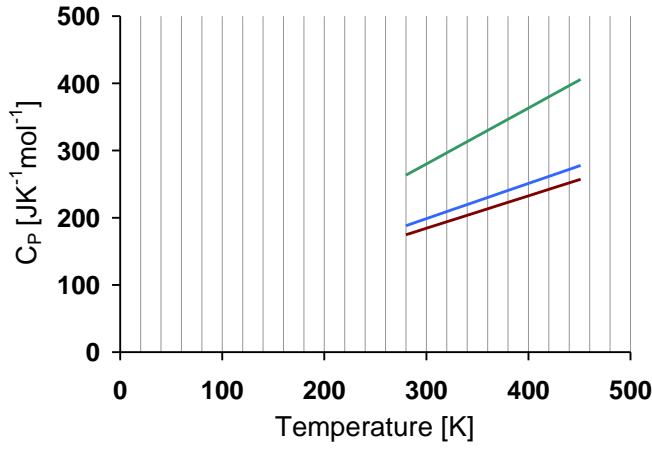


**Figure 8.** Experimental heat capacity of form I (red), form II (blue), extrapolated to the melting points, and calculated heat capacity of the supercooled melt (green).

It is now possible to use the derived temperature dependence of  $\Delta C_p$  to evaluate the thermodynamic stability relationship from 280 K up to the melting temperature of the two polymorphs. The van't Hoff plot in figure 9 shows the temperature – activity relationship of the two polymorphs, calculated using eq. 3 and 5, from ambient temperature up to their respective melting points. The stability transition temperature is 156.1°C (429.3 K) if eq. 5 and the parameters in table 7 are used, compared to 155.8°C if eq. 6 is used, and  $\leq 157.25^\circ\text{C}$  according to DSC observations of the solid-solid transition.

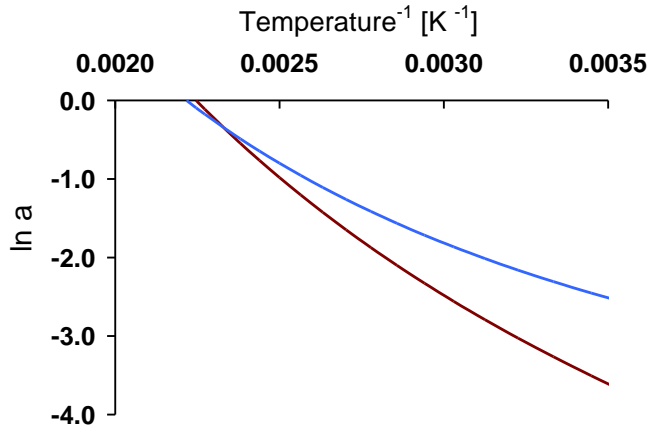


**Figure 9.** The solid-state activity of form I (red) and form II (blue) from 280 K up to the melting temperature of each polymorph.

Furthermore, real energy-temperature diagrams can now be constructed, describing the temperature dependence of the Gibbs free energy of fusion,  $\Delta G^f(T)$ , the enthalpy of fusion,  $\Delta H^f(T)$ , and the entropy of fusion,  $\Delta S^f(T)$ , for each polymorph. Based on eq. 3 and 5 the following thermodynamic relations can be derived from the melting temperature, at which the chemical potential of the solid is equal to the chemical potential of the melt:

$$\Delta G^f(T) = \Delta H^f(T_m) \left[ 1 - \frac{T}{T_m} \right] + q \left[ T - T_m - T \ln \left( \frac{T}{T_m} \right) \right] + r \left[ \frac{T^2}{2} - \frac{T_m^2}{2} - T_m T \ln \left( \frac{T}{T_m} \right) \right] \quad (7)$$

$$\Delta H^f(T) = \Delta H^f(T_m) + q(T - T_m) - \frac{r}{2}(T - T_m)^2 \quad (8)$$

$$\Delta S^f(T) = \Delta S^f(T_m) + q \ln\left(\frac{T}{T_m}\right) + r \left[ T_m \ln\left(\frac{T}{T_m}\right) - T + T_m \right] \quad (9)$$

The complete thermodynamic relationship of the two polymorphs determined using eq. 7 - 9, are shown in figure 10.

As can be seen in figure 10, the magnitude of both the enthalpy and entropy term is consistently lower for form II than for form I over the entire investigated temperature interval. The polymorphic stability transition appears at 429.3 K at which point the enthalpy difference between form II and form I is 9.2 kJ·mol<sup>-1</sup> and the entropy difference is 21.4 J·mol<sup>-1</sup>·K<sup>-1</sup>. With decreasing temperature, the enthalpy difference between form II and form I decreases down to 6.7 kJ·mol<sup>-1</sup> at 280 K, and the entropy difference is reduced to 14.5 J·mol<sup>-1</sup>·K<sup>-1</sup>, corresponding to a TΔS contribution to the difference in free energy of 4.0 kJ·mol<sup>-1</sup>. It is also seen in figure 10 that ΔG<sup>f</sup>(T) approaches ΔH<sup>f</sup>(T) with decreasing temperature, for both polymorphs. The ΔG and ΔH-curves will theoretically converge at 0 K, and, as can be seen in figure 10, this can be expected to occur somewhere between 8.7 – 16.1 kJ·mol<sup>-1</sup> for form I and between 6.0 – 9.4 kJ·mol<sup>-1</sup> for form II.

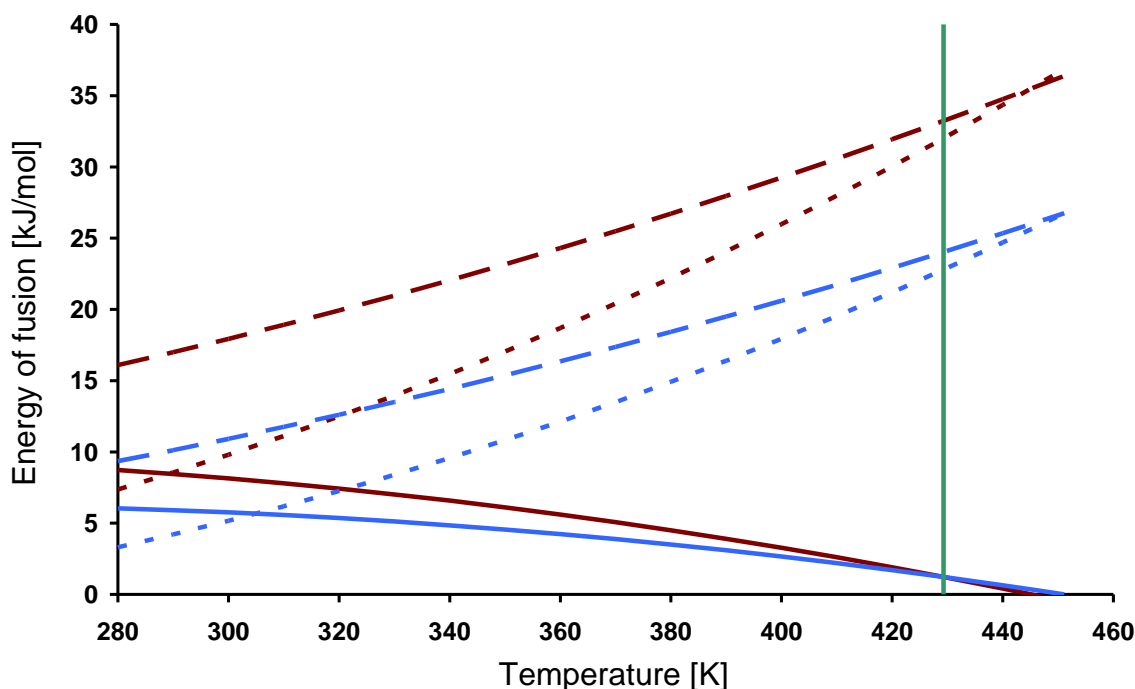


**Figure 10.** Energy of fusion-temperature diagram of form I (red) and form II (blue), displaying how the thermodynamic properties ΔG<sup>f</sup> (solid curves), ΔH<sup>f</sup> (dashed curves) and T·ΔS<sup>f</sup> (dotted curves) change with temperature up to the melting temperature of respective polymorph. The polymorphic transition temperature is given as a green vertical line at 429.3 K.

#### *Primary nucleation of mABA polymorphs*

In analysing the nucleation results in table 5, the average supersaturation ratio with respect to the thermodynamically stable polymorph (form I) at the onset of nucleation, S<sub>I</sub>, is given for each series of nucleation experiments:

$$S_I = \frac{x}{x_{I,eq}} \quad (10)$$

where  $x$  represents the mole fraction concentration of mABA in solution and  $x_{I,eq}$  is the corresponding mole fraction solubility of form I at the nucleation temperature. For acetonitrile and ethyl acetate, the solubility of form II has been determined experimentally, and the corresponding average supersaturation ratio is also given in table 5. However, since the solubility of form II could not be measured in water or methanol, for the purpose of further analysis the approximation that the solubility ratio of the two polymorphs in a solvent is independent of the solvent is employed. The rationale for this is as follows:

The mole fraction solubility of the solid phase  $i$  at a given temperature can be written as:

$$x_{eq,i} = \frac{a_i}{\gamma_{eq}} \quad (11)$$

The solubility ratio of form II to form I at that temperature then becomes:

$$\frac{x_{eq,II}}{x_{eq,I}} = \frac{a_{II}}{a_I} \frac{\gamma_{eq,I}}{\gamma_{eq,II}} \quad (12)$$

The activity coefficient  $\gamma$  depends on solvent, temperature and solution concentration but is independent of the solid phase structure. In eq. 12, the ratio of activity coefficients captures the entire influence of the solvent on the solubility ratio of the two polymorphs. In the same way, the ratio of solid-state activities accounts completely for the influence of the solid forms on the solubility ratio, except for the fact that the different forms have different solubility, which effects the activity coefficient ratio via the concentration dependence of the activity coefficient. In figure 11, the solubility ratio of the two polymorphs in ethyl acetate and acetonitrile, respectively, are plotted in the temperature interval 5 – 30°C, corresponding approximately to where experimental solubility data is available. In addition, the ratio of solid-state activities of the two polymorphs is shown. For these two solvents, the solubility ratios are quite similar, differing only by 4.5 – 10%. Furthermore, in this temperature interval the ratio of solid-state activities is close to the solubility ratios and the relationship between solubility ratio and solid-state activity ratio is approximately linear with temperature.

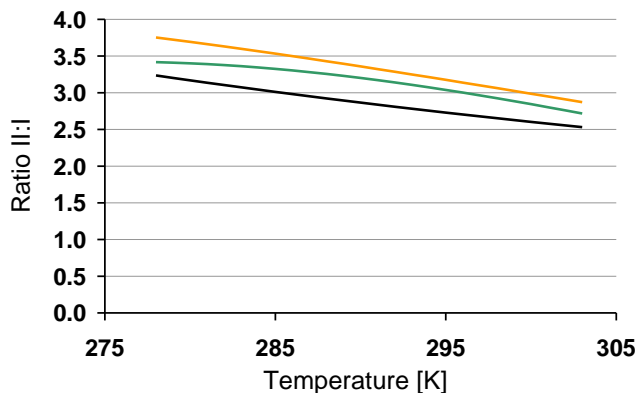


**Figure 11.** The ratio of the solubility of form II to that of form I in ethyl acetate (orange) and acetonitrile (green), and the corresponding ratio of solid-state activities (black).

As shown in figure 11, in acetonitrile and ethyl acetate the ratio of activity coefficients is reasonably close to unity, and accordingly the influence of concentration on the activity coefficient is not large. Based on figure 11, no dramatic difference in the solubility ratio between different solvents is expected, because this ratio is expected to, and appears mainly to be governed by the ratio of solid-state activities.

In figure 12 is shown the mole fraction solubility of the two polymorphs in the different solvents, as well as the solid-state activities (ideal solubility), in a van't Hoff plot.

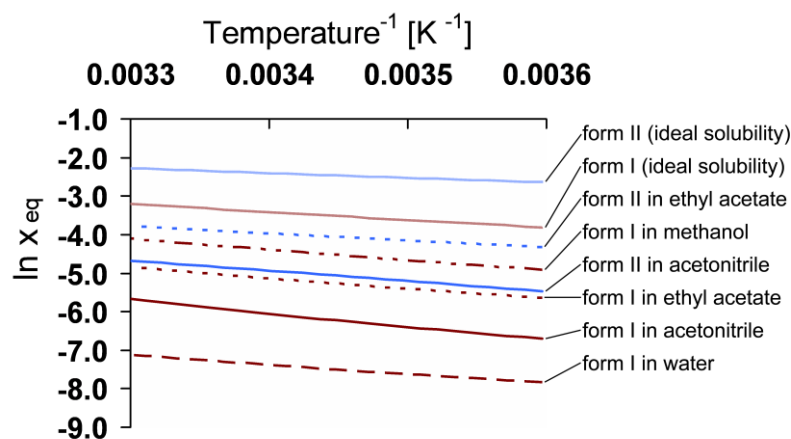


**Figure 12.** A van't Hoff plot of the solubility of the two polymorphs in the temperature interval 5 – 30°C.

The mole fraction solubility in methanol is comparatively high, then follows the solubility in ethyl acetate, acetonitrile and finally water in which the solubility is fairly low. Based on figure 12 there is no particular reason to expect that the solubility ratio between the two polymorphs in water and, especially, in methanol would differ significantly from that in ethyl acetate and acetonitrile. Hence, all in all it appears to be a reasonable approximation to assume that the solubility ratio is independent of the solvent, and below the solubility of form II in methanol and water is estimated using the average solubility ratio in acetonitrile and ethyl acetate at each temperature.

As mentioned earlier, the solid material generated in the nucleation experiments was filtered and analyzed immediately upon visible nucleation, as semi-dry material with no specific drying step. Throughout the following discussion, it will be assumed that the polymorph identified in the sample is also the polymorph that actually nucleated. However, in some experiments there is the possibility that the observed polymorph is actually the result of a transition following the nucleation. In methanol, only form I was observed and all nucleation occurred while the solution was undersaturated with respect to form II according to the above analysis, so in this case there is no uncertainty regarding the nucleating polymorph. In water, some experiments nucleated above the solubility curve of form II, and even though all experiments produced form I, there is a possibility in these cases that the nucleating polymorph was form II. It should be noted that we have no observations that support this, but on the other hand we have observed that the transformation of form II into form I is rapid in aqueous solution. In acetonitrile, most experiments produced form II. In the slurry solutions of form II in acetonitrile used for measuring the solubility of this polymorph, no detectable transformation occurred for significant periods of time at low temperatures. Hence, we have fairly strong reasons to believe that in the experiments where form I was isolated, this is also the form that nucleated.

In figure 13, the primary nucleation events observed in the different solutions are plotted in concentration – temperature graphs, together with the solubility curves of the two polymorphs. In acetonitrile, the nucleation occurs at a temperature where the solution is supersaturated with respect to both polymorphs, and 83% of the nucleation experiments resulted in form II. In methanol only form I nucleated, and as shown in figure 13 it appears that all nucleation events in this solvent occurred while the solution was clearly undersaturated with respect to form II. The interpretation is that in acetonitrile,

the metastable zone of form I is so wide as to allow cooling to proceed into the region where form II also becomes supersaturated before nucleation occurs, while in methanol the metastable zone of form I is much more narrow. In water, just like in methanol, form I nucleated in 100% of the experiments, and again, although less clear than for methanol, our estimate of the solubility of form II suggests that in water, nucleation took place at temperatures where the solution was undersaturated, or just slightly supersaturated, with respect to form II.

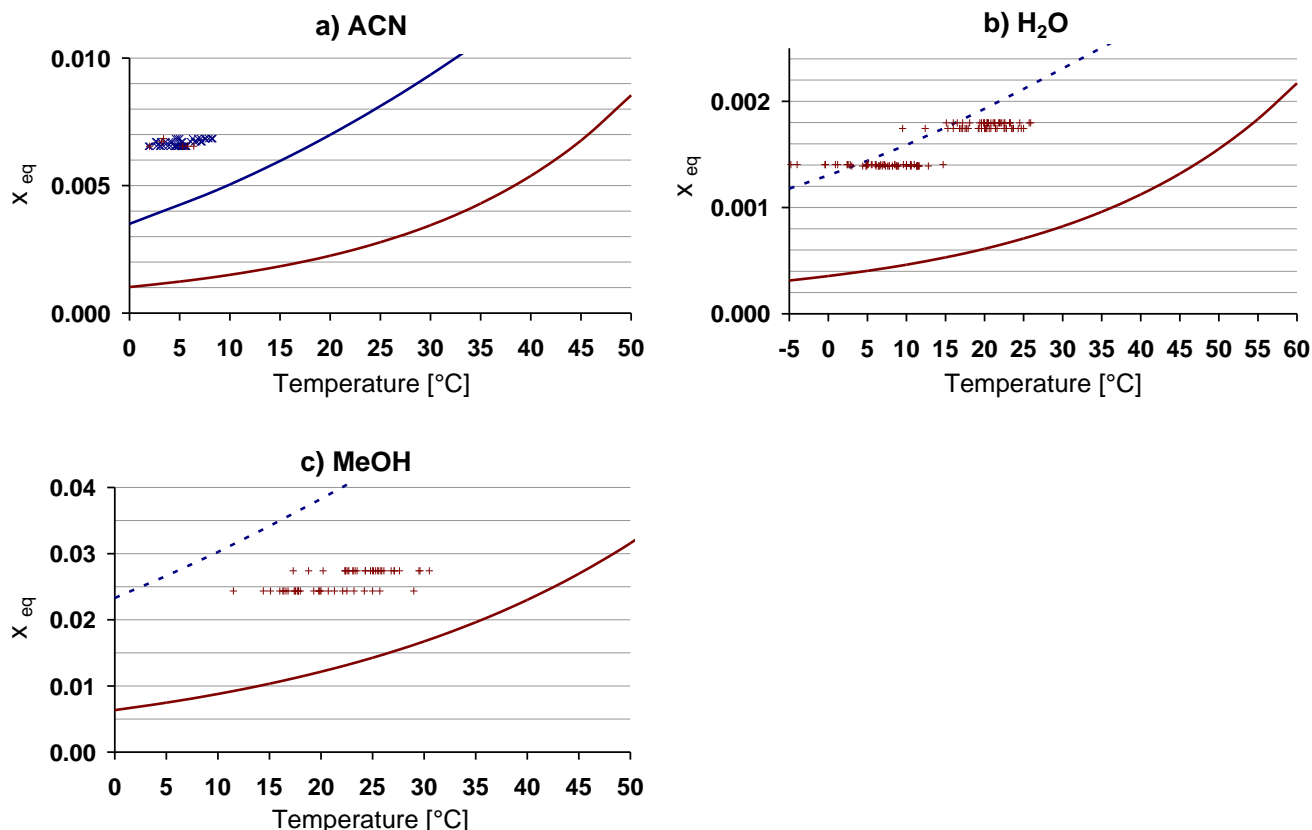


**Figure 13.** The onset of nucleation plotted in a concentration vs. temperature graph, together with solubility curves, for form I (red) and form II (blue), in a) acetonitrile, b) water, and c) methanol. The solubility of form II in water and methanol was estimated using the average solubility ratio between the two forms in acetonitrile and ethyl acetate (dashed curves).

Overall, it appears that it is comparatively more difficult for a stable nucleus of form I to form in acetonitrile than in methanol. In ethyl acetate, finally, the conditions are such that, when the experiments were aborted at the low-temperature limit, the solutions were not sufficiently supersaturated for either form to nucleate –  $S_I$  was then at 4.9 and  $S_{II}$  at 1.3, indicating that the metastable zone of form I in this solvent is considerable. This is further illustrated by figure 14, where the polymorphic outcome of nucleation experiments under different experimental conditions are shown against the supersaturation ratio with respect to form II. This diagram clearly shows that for the majority of experiments resulting in form I, nucleation occurred while form II was still undersaturated.

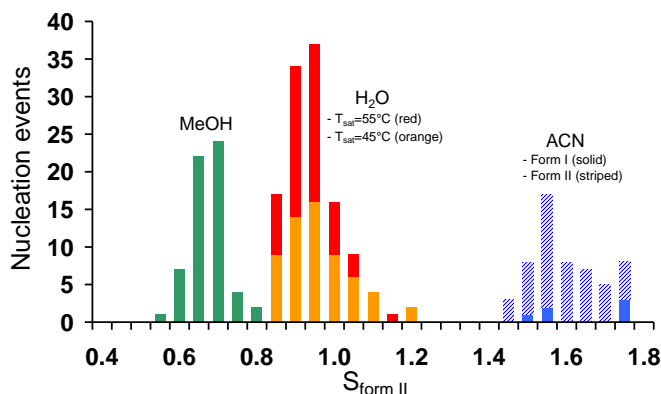


**Figure 14.** The number of samples nucleating at different intervals of relative supersaturation, with respect to form II.

The nucleation of form I, as given by figures 13 and 14, is much more difficult in acetonitrile and ethyl acetate than in water and methanol. The crystal structure of form I has not been resolved, which is unfortunate for a discussion of the structure-nucleation relationship. However, it has been reported that this polymorph is a zwitterionic structure<sup>6,7</sup>, whereas in form II the molecules are non-ionic. Accordingly, the nucleation of form I is expected to depend on the concentration of zwitterions in solution. The distribution between zwitterions and non-ionic molecules is expressed by the equilibrium constant  $K_Z$ :

$$K_Z = \frac{\{^+H_3N - Ar - COO^-\}}{\{H_2N - Ar - COOH\}} \quad (13)$$

It has been reported<sup>11,12,13</sup> that values of  $K_Z$  for aminobenzoic acids in water are in the order of unity, in marked contrast to simple, aliphatic amino acids which tend to exist almost completely in the zwitterionic form in aqueous solution. In water at room temperature conditions, mABA has been reported by different authors to be 50%<sup>11</sup> and 70%<sup>12</sup>, respectively, in zwitterionic form. Unfortunately, we have not been able to find distribution coefficients for mABA in the other solvents investigated, but in dioxane and chloroform it has been shown that mABA is largely present in its non-ionic form in solution<sup>6</sup>. In general,  $K_Z$  will depend on the capacity of the solvent molecules to solvate and stabilize the two molecular forms<sup>14</sup>. Investigations of the zwitterionic : non-ionic equilibrium of the solvatochromic dye rhodamine B in different solvents have shown that mainly the protic character of the solvent, but also the polarity, as well as the temperature, can be correlated to the distribution in solution between zwitterions and non-ionic molecules<sup>15</sup>. The same study also reports that the zwitterion concentration of rhodamine B in acetonitrile and ethyl acetate solutions is virtually zero.

Accordingly, a probable explanation for the influence of the solvent on the nucleation of form I is that methanol and water are polar, protic solvents, containing hydroxyl groups that can form hydrogen bonds with, and thus stabilize, a zwitterionic molecule in solution. In these solvents there may thus be a fair concentration of the zwitterionic form, which would facilitate the nucleation of form I. Acetonitrile and ethyl acetate, however, are aprotic solvents, and hence by the same argument poor solvents for a zwitterionic form. The concentration of zwitterions can thus be expected to be very low, and the nucleation of form I to be significantly more difficult. Finally, it is perhaps unexpected to find that form I is able to nucleate more easily in methanol than in water. However, for rhodamine B it is reported<sup>15</sup> that the compound in methanol is slightly more dissociated than in water. In addition, the mole fraction solubility of mABA is approximately 18 times higher in methanol than in water.

As figure 13 shows, the spread in nucleation with respect to temperature is considerable in all solvents. If the data is instead considered with respect to the thermodynamic driving force required for nucleation, expressed for the solid form  $i$  as the difference in the chemical potential of the solute in solution at the point of nucleation compared to saturation at the same temperature:

$$\Delta\mu_i = RT \ln \frac{\gamma}{\gamma_{eq,i}} \frac{x}{x_{i,eq}} \cong RT \ln \frac{x}{x_{i,eq}} = RT \ln S_i \quad (14)$$

it can be seen in figure 15 that the spread in nucleation in terms of driving force is on the order of one kJ/mol. For form I, the spread appears to decrease with increasing driving force. Equation 14 assumes that the influence of small concentration differences on the activity coefficient can be neglected.

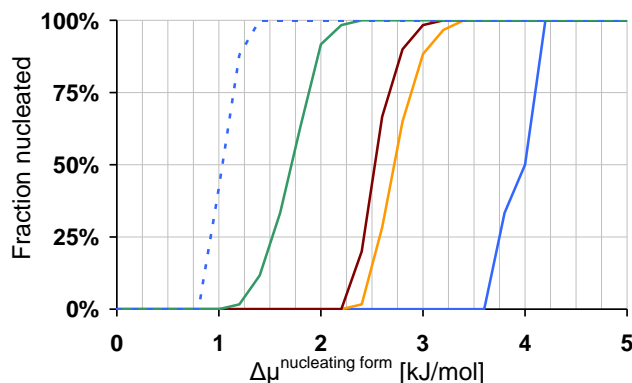


**Figure 15.** Cumulative distribution of nucleation events vs. increasing thermodynamic driving force for nucleation, expressed in terms of difference in solute chemical potential between the solution at nucleation and at equilibrium, with respect to the nucleating polymorph: methanol,  $T_{sat}=45^{\circ}\text{C}$  (green); water,  $T_{sat}=55^{\circ}\text{C}$  (red) and  $T_{sat}=45^{\circ}\text{C}$  (orange), and acetonitrile,  $T_{sat}=45^{\circ}\text{C}$ , (blue, form I = solid curve, form II = striped curve).

For a polymorphic system, the case of *m*-aminobenzoic acid shows how the solid phase that nucleates depends on the relationship between thermodynamics and kinetics. In order to achieve control over the crystallizing polymorph, it is necessary to consider solubility relationships as well as nucleation kinetics of each polymorph, and in addition how the speciation in solution relates to how the compound appears in the solid state. At any point during a crystallization, any polymorph whose current solubility is lower than the solution concentration has the potential to nucleate, and whether it will do so or not is governed by kinetics. In order for the metastable form to appear, a more narrow metastable zone is not sufficient; the metastable form may only nucleate if the nucleation of the stable form is sufficiently obstructed, in relation to the difference in solubility between the two polymorphs. For *m*-aminobenzoic acid, form I is thermodynamically much more stable than form II. However, in acetonitrile, the nucleation of form I is quite difficult, whereby form II can be given the opportunity to become supersaturated and nucleate. In methanol in particular, but also in water, the metastable zone of form I is more narrow compared to the difference in solubility between the two polymorphs, and only form I nucleates. Of course, it is important to recognize that in general, the solubility of a metastable polymorph may not always be easy to determine. Furthermore, the mechanisms of molecular clustering and nucleation of a solid in solution are poorly understood<sup>16</sup> and not easily investigated.

The experimental results of the present work clearly illustrate the stochastic nature of primary nucleation. Not only is there a significant spread in nucleation temperature in all the solvents; in acetonitrile there is also a variation in the polymorph that nucleates. In 83% of the experiments, form II is obtained, in 10% form I, and in 7% the result is a concomitant nucleation of the two polymorphs.

## CONCLUSIONS

*m*-Aminobenzoic acid can crystallize into two different polymorphs. The polymorphs are enantiotropically related, with a transition temperature determined by calorimetry to be below  $157.25^{\circ}\text{C}$ , and by a thermodynamic analysis to be  $156.1^{\circ}\text{C}$ . At ambient temperature, form I is the

thermodynamically stable form. The only published structure<sup>5</sup> is actually that of form II, which is strongly metastable at ambient conditions.

The thermodynamic parameters free energy, enthalpy and entropy of fusion have been determined as functions of temperature, for both polymorphs, by a comprehensive thermodynamic analysis. The energy – temperature diagram reveals an enthalpy difference between form II and form I of 9.2 kJ·mol<sup>-1</sup> at the transition temperature, decreasing to 6.7 kJ·mol<sup>-1</sup> at 280 K.

The study of primary nucleation has shown that for mABA, the polymorph that nucleates depends on the solvent. By performing multiple identical cooling crystallization experiments at different conditions, it has been shown that in spite of a large difference in solubility at the investigated temperatures, it is possible to produce the metastable form II by choosing conditions where the crystallization kinetics strongly favour this polymorph over the stable form I. In 60 identical experiments with acetonitrile solutions saturated at 45°C, 83% resulted in pure form II, and 17% either in pure form I or in a mixture of the two polymorphs. However, in methanol in particular, but essentially also in water, the metastable zone of form I is too narrow, in comparison to the difference in solubility, to allow form II to nucleate. It has been reported that the solid form of m-aminobenzoic acid here referred to as form I is composed of zwitterions<sup>6,7</sup>. Since the concentration of zwitterions in solution can be expected to very low in acetonitrile and ethyl acetate this explains the relative difficulty of nucleating form I in these solvents. This work underlines the importance of investigating both thermodynamic and kinetic aspects of the system, in order to clearly establish and rationalize the conditions of appearance of different polymorphs. The work also illustrates the important implications of the stochastic nature of nucleation for a polymorphic system, and the need to account for this in experimental work.

## REFERENCES

- (1) Henck, J. O.; Griessner, U. J.; Burger, A. Polymorphie von Arzneistoffen. *Pharm. Ind.* **1997**, 59(2), 165.
- (2) Kuhnert-Brandstätter, M.; Sollinger, H. W. Thermal analytical and infrared spectroscopic investigations on polymorphic organic compounds – V. *Mikrochim. Acta* **1989**, 99, 125.
- (3) Byrn, S.; Pfeiffer, R.; Ganey, M.; Hoiberg, C.; Poochikian, G. Pharmaceutical solids: a strategic approach to regulatory considerations. *Pharm. Res.* **1995**, 12(7), 945.
- (4) Alcolea Palafox, M.; Gil, M.; Núñez, J. L. Meta-aminobenzoic acid: structures and spectral characteristics. *Spectrosc. Lett.* **1996**, 29, 609.
- (5) Voogd, J.; Verzijl, B. H. M.; Duisenberg, A. J. M. m-Aminobenzoic acid. *Acta Crystallogr.* **1980**, B36, 2805.
- (6) Gopal, L.; Jose, C. I.; Biswas, A. B. Infra-red spectrum and zwitterion structure of meta aminobenzoic acid. *Spectrochim. Acta* **1967**, 23A, 513.
- (7) Théorêt, A. Structure moléculaire et zwitterion des acides aminés – I. *Spectrochim. Acta* **1971**, 27A, 11.
- (8) Burger, A.; Ramberger, R. On the polymorphism of pharmaceuticals and other molecular crystals I. *Microchim. Acta* **1979**, II, 259.
- (9) Nordström, F. L.; Rasmuson, Å. C. Determination of the activity of a molecular solute in saturated solution. *J. Chem. Thermodyn.* **2008**, 40, 1684.
- (10) Nordström, F. L.; Rasmuson, Å. C. Prediction of solubility curves and melting properties of organic and pharmaceutical compounds. *Eur. J. Pharm. Sci.* **2009**, 36, 330.
- (11) Kumler, W. D. Acidic and basic dissociation constants and structure. *J. Org. Chem.* **1955**, 20, 700.
- (12) Cohn, E. J.; Edsall, J. T. *Proteins, amino acids and peptides*, chapter 4; Reinhold Publishing Corporation: New York, **1943**.
- (13) Bjerrum, N.; Die Konstitution der Ampholyte, besonders der Aminosäuren, und die Dissoziationskonstanten. *Z. Physik. Chem.* **1923**, 104, 147.
- (14) Reichardt, C. *Solvents and solvent effects in organic chemistry*; Wiley-VCH Verlag: Weinheim, **2003**.
- (15) Hinckley, D. A.; Seybold, P. G.; Borris, D. P. Solvatochromism and thermodynamics of rhodamine solutions. *Spectrochim. Acta* **1986**, 42A, 747.
- (16) Gavezzotti, A. *Molecular aggregation*; Oxford University Press: New York, **2007**.